

How Stride Adaptation in Pedestrian Models Improves Navigation

Isabella von Sivers*, Gerta Köster

Munich University of Applied Sciences, Lothstraße 64, 80335 Munich, Germany

Abstract

Pedestrians adjust both speed and stride length when they navigate difficult situations such as tight corners or dense crowds. They do this with foresight reacting instantly when they encounter the difficulty. This has an impact on the movement of the whole crowd especially at bottlenecks where slower movement and smaller steps can be observed. State-of-the-art pedestrian motion models automatically reduce speed in dense crowds simply because there is no space where the virtual pedestrians could advance. The stride length, however, is rarely considered, which leads to artifacts. We reformulate the problem of correct stride adaptation as an optimization problem on a disk around the pedestrian. He or she seeks the position that is most attractive in a sense of balanced goals between the search for targets, the need of space of individual pedestrians and the need to keep a distance from obstacles. The result is a fully automatic adjustment that simplifies calibration, and gives visually natural results and an excellent fit to measured experimental data.

Keywords: Pedestrian Movement, Crowd Dynamics, Optimal Steps Model, Stride Length Adaptation, Optimization, Nelder Mead Simplex

1. Introduction

Simulation of pedestrian movement becomes increasingly important to ensure safety for everybody wherever a crowd comes together, e.g. at urban

*Corresponding author, Tel.: +49-89-1265-3762

Email addresses: isabella.von_sivers@hm.edu (Isabella von Sivers),
gerta.koester@hm.edu (Gerta Köster)

events. Many new models for pedestrian dynamics have been presented over the last years and existing models are being constantly refined [9, 37, 32, 28]. Among them cellular automata [2, 17, 14, 8] and social force models [13, 11, 4, 21] are prominent and, perhaps, best investigated. But some typical aspects of human movement are still missing in known models, in particular the immediate adaptation of the stride length to the navigational situation.

When pedestrians navigate a difficult corner or walk within a crowd they reduce their speed. And more than that, they make smaller steps. They do this with foresight, that is, they adapt to the situation before or at the moment they encounter it. Some current state-of-the-art pedestrian motion models are capable of speed adaptation, typically in a reactive way, but do not adjust the stride length [28]. In fact, standard continuous models, based on differential equations, do not even model steps but a sliding motion along imaginary rails. Cellular automaton models only allow ‘hops’ from one cell to the next. Stride adaptation is impossible. In this paper, we present a model that fully models step-wise movement with immediate stride length adaptation, thus matching human walking much more closely. This leads to visually more natural results, easier calibration and excellent fit with measured data from well known experiments.

Our model further develops the Optimal Steps Model (OSM), one of the newer approaches to modeling pedestrian dynamics introduced in [28]. The OSM is inspired by the rule based approach of cellular automata models, in particular the rules of the model described in [20]. However, movement is not restricted to a grid. The next position of a pedestrian is chosen on a circle around the pedestrians midpoint. The radius of the circle represents the stride length. In [28] two ways to determine the stride length are described: The simpler approach is to fix the stride length in accordance to the pedestrian’s free-flow velocity. This means that there is no stride length adaptation during simulation. The second approach is to relate the stride length to the actual speed. Since the speed must be measured using positions from the past this approach suffers from a delay in adaptation.

In this paper we present a simple extension of the OSM that enables immediate stride length adaptation: We search the next position on a disk instead of a circle. The change seems small at first but the impact is significant: With this improvement, we can show more realistic movement of the virtual pedestrians and it allows, in contrast to the prior state of the art, to calibrate to measured density-speed relations by adjusting only a single and plausible parameter in our model.

The paper is structured as follows: Section 2 gives a short introduction to tactical path-finding in the Optimal Steps Model. In section 3 we formulate the choice of the direction and length of the next step as a non-linear optimization problem on a disc. Section 4 shows how we solve the optimization problem numerically. Section 5 gives several typical tests scenarios, like flow through a bottleneck, to highlight how the new stride length adaptation improves on former models. Section 6 evaluates the results and gives an outlook on next steps.

2. Navigation in the Optimal Steps Model

In the Optimal Steps Model [28], pedestrians seek targets and avoid other pedestrians and obstacles. They navigate along a floor field constructed by superposing scalar fields. The three scalar functions express the orientation towards a target, the need to avoid too close contact with fellow pedestrians and the need to skirt obstacles.

The historical way to look at these functions is to think of them as potentials that, through the potentials' gradients, represent forces between the target, the pedestrians and the obstacles. This inspiration from physics has produced the older model generation including social force models. However, in reality, there are no such forces. Also, the OSM does not use the gradients of the scalar field at all but follows the idea of a utility function. Utility functions better match the proposition that persons seek advantageous decisions described in modern cognition models [1]. Thus we believe that the terms 'potential' and 'force' may mislead the reader by introducing wrong analogies.

The 'target orientation' is given by a wave front propagating from the target (see Fig. 1) as suggested in [33, 10]. Let $\Omega \subset \mathbb{R}^2$ be the area of

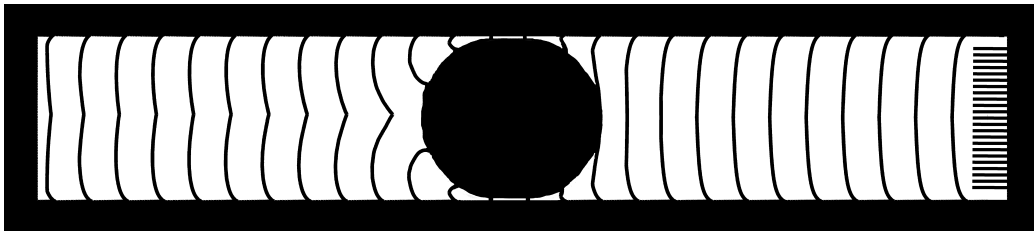


Figure 1: Wave front propagating from the target (horizontally striped, on the right) around a pillar within a corridor.

observation of the scenario with boundary $\partial\Omega$. $\Gamma \subset \partial\Omega$ denotes the boundary of the target. We assume that each pedestrian tries to choose the path with the shortest travel time to the target. The solution of the Eikonal equation (1) gives the arrival time $\Phi : \Omega \rightarrow \mathbb{R}$ of a wave front that propagates through space starting from Γ . The traveling speed of the front is given by $F : \Omega \rightarrow \mathbb{R}_+$. Typically, F is chosen to be 1 outside obstacles making the arrival time independent of surface conditions. More difficult terrain can easily be mapped by varying F [10]. The Eikonal equation is given by

$$F(x)\|\nabla\Phi(x)\| = 1 \quad \text{for } x \in \Omega \quad (1)$$

with boundary condition

$$\Phi(x) = 0 \quad \text{for } x \in \Gamma. \quad (2)$$

The numerical solution $\tilde{\Phi}(x)$ is efficiently computed by Sethian's fast marching algorithm on a two-dimensional grid [29, 30]. We interpolate $\tilde{\Phi}(x)$ bilinearly between grid points [10, 28] to define the 'target orientation' $P_t(x)$ for every point $x \in \Omega$.

In addition to the static 'target orientation', the floor field contains dynamic 'pedestrian avoidance' and 'obstacle avoidance'. The formulas are taken from [28].

The 'pedestrian avoidance' (see Fig. 2) determines how large the personal space around a pedestrian is. It is given by function

$$P_p^j(x) := \begin{cases} \mu_p & \text{if } \delta_p^j(x) \leq g_p, \\ \nu_p \cdot \exp[-a_p \cdot \delta_p^j(x)^{b_p}] & \text{if } g_p < \delta_p^j(x) \leq g_p + h_p, \\ 0 & \text{else.} \end{cases} \quad (3)$$

$P_p^j(x)$ only depends on the Euclidean distance $\delta_p^j(x)$ between the center of pedestrian j and the considered position x . g_p is the torso diameter of the pedestrian. At this point it is identical for all pedestrians. We prevent the virtual pedestrians from overlapping by setting the avoidance value to an extremely high value μ_p inside each torso area. For better computational speed, we cut off outside a radius of influence $g_p + h_p$. The strength of the avoidance of a pedestrian can be controlled by adjusting the parameters ν_p , a_p and b_p .

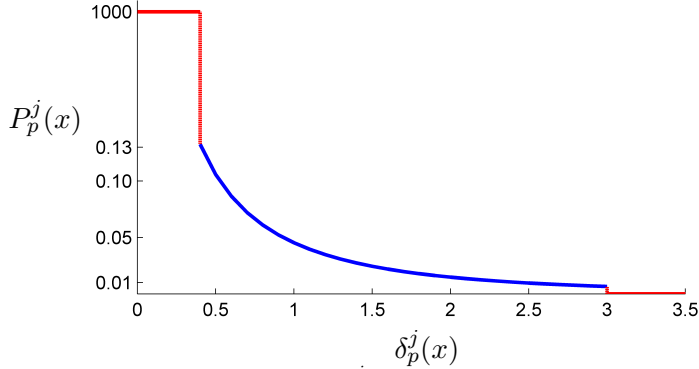


Figure 2: The 'pedestrian avoidance' P_p^j of pedestrian j in position x depends on the distance of x to the pedestrian's midpoint.

The 'obstacle avoidance'

$$P_o^k(x) := \begin{cases} \mu_o & \text{if } \delta_o^k(x) \leq g_p/2, \\ \nu_o \cdot \exp[-a_o \cdot \delta_o^k(x)^{b_o}] & \text{if } g_p/2 < \delta_o^k(x) \leq h_o, \\ 0 & \text{else,} \end{cases} \quad (4)$$

is very similar to the way we compute the avoidance value of a pedestrian. In this case, $\delta_o^k(x)$ is the Euclidean distance between the considered position x and the closest point of the obstacle k . We set the function to a high value μ_o within the obstacle area to avoid virtual people from walking into obstacles. We cut it off when $\delta_o^k(x) > h_o$. Again, the 'obstacle avoidance' can be controlled by changing ν_o , a_o and b_o .

For each pedestrian i the superposition

$$P_i(x) = P_t(x) + \sum_{j=1, j \neq i}^n P_p^j(x) + \sum_{k=1}^m P_o^k(x), \quad (5)$$

constitutes the floor field $P_i(x)$ for any point $x \in \Omega$ [28].

3. Mathematical formulation of stride adaptation as a two-dimensional optimization problem

We interpret the floor field, or rather its negative, as an utility function or an objective function for pedestrian i . The closer to the target and the farther away from obstacles and other pedestrians the more attractive is the position. Function $-P$ measures the degree of the attraction or P the degree of 'repulsion' or 'discomfort'.

As a consequence we require that, with each step, each virtual pedestrian selects the position with the lowest value of the floor field within his or her reach. In the original model formulation [28], the next position is chosen on a circle with radius r around the pedestrian that represents the individual’s stride length. Thus, the floor field was the objective function of an one-dimensional minimization problem where the position on the circle with the lowest value has to be found. The pedestrian moves if, and only if, the candidate position on the circle has a lower floor field value than the one at the actual position.

Optimizing on the circle already significantly improved on the state-of-the-art in 2012 [28] but did not allow for immediate stride length adjustment according to the current situation. We remedy this shortcoming by searching the next position on a disc with radius r instead of a circle around the pedestrian [34]. This leads to a two-dimensional optimization problem with one inequality constraint:

$$\begin{aligned} & \min_{x \in \Omega} P_i(x) \\ \text{s.t.} \quad & \delta_p^i(x) - r \leq 0 \end{aligned} \quad (6)$$

Note that with our choice of the floor field the objective function P_i (5) is nonlinear, not differentiable and discontinuous.

4. Numerical solution

To find the minimum on the disc, we use a well known and effective algorithm for optimization problems with a discontinuous objective function: The Nelder-Mead simplex algorithm [25] is a local direct search method for unconstrained optimization where no gradient information is available. It is usually applied to minimization problems.

For functions on \mathbb{R}^n , the algorithm starts with an initial simplex S_0 constructed by $n + 1$ vertices x_0, \dots, x_n . The Nelder-Mead method modifies and improves the simplex in every loop using four operations: reflection, expansion, contraction, and shrinkage. These operations are managed by four parameters: α (reflection coefficient), β (expansion coefficient), γ (contraction coefficient), and δ (shrinkage coefficient) which satisfy $\alpha > 0, 0 < \beta < 1, \gamma > 1, \gamma > \alpha, 0 < \delta < 1$.

Convergence of the Nelder-Mead algorithm is sensitive to the choice of the initial simplex and cannot be guaranteed in general but, in practice, it

provides good results in low dimensions regardless of the objective function [22]. This is confirmed by our results [34]. When we compare the Nelder-Mead method to a straight forward search on a grid and to evolutionary algorithms Nelder-Mead proves to be the fastest and most accurate method of these [34]. For our applications, the method never failed to converge with only five starting simplices, one at the center of the disc and four rotating on the circle around the pedestrian.

5. Validation

To validate a model means to show that it matches reality as far as necessary to achieve the modeling goal. In our case we wish to build models that give qualitatively and, to a certain extent, quantitatively realistic predictions of possibly dangerous situations within a moving crowd. In particular, dangerously high crowd densities should be well resolved. When safety of life and limb is at task, we feel that validation must be handled strictly. Hence, within our VADERE simulation platform, every model we investigate is checked against the tests listed in the RiMEA validation guideline [26] with the exception of those test where we do not claim to model the situation, e.g. movement on several levels of a building. Hence, not only the OSM is tested in this way but also the implementations of a social force model and a cellular automaton model that we use for comparison [28, 7].

We take a closer look at two scenarios where experimental data is available.

- Navigation around a column in narrow corridor inspired by the experiment in [24].
- The density-speed relationship expressed through fundamental diagrams. Here we go beyond the qualitative match required in the RiMEA guideline test 10. We demand that the model is capable of calibrating to any measured density-speed relation.

5.1. Navigation around a column in a corridor

In this scenario a column is placed in the middle of a narrow corridor so that there is barely enough space for the pedestrians to pass the column. Single pedestrians walk from left to right. From the experiment in [24], where the column was emulated by a person, we expect trajectories that,

when aggregated, form an ‘eye’ around the column. The steps themselves, unfortunately, were not resolved in the laboratory experiment.

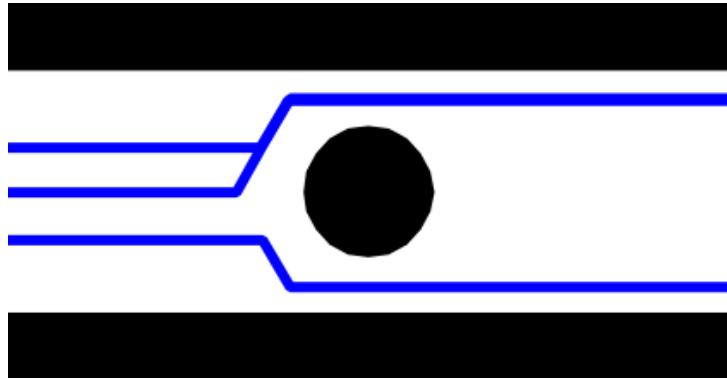
Fig. 3 compares the trajectories of ten virtual pedestrians of three models: a cellular automaton model on a hexagonal grid, the OSM with optimization on a circle with radius $r =$ stride length from [28] and the OSM with stride adaptation through optimization on the disc with radius $r =$ maximum stride length from [34]. The pedestrians start one after another so that they do not impede each other. In Fig. 3(a) we clearly see the artifact caused by the underlying grid. Fine navigation cannot be resolved at all. The OSM in its original version significantly improves on that, but the step lengths remain unnaturally big in the confined space next to the column. Also the trajectories still seem somewhat coarse (Fig. 3(b)). The OSM model with the natural stride adaptation performs best with smoother but not completely smooth trajectories (Fig. 3(c)) which, in our eyes, is how people walk in reality.

The case where several persons move at the same time is demonstrated in Fig. 4 for the OSM with fixed and adaptive stride length.

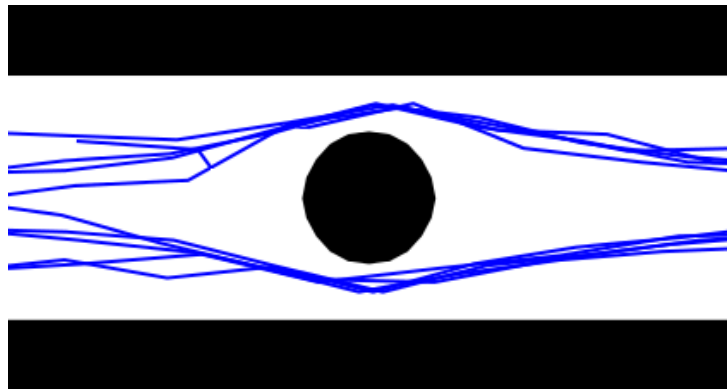
For the cellular automaton model, pedestrians sometimes get stuck in front of a narrowing if there is no free cell between the column and the wall. This can be mitigated by carefully positioning the obstacles on the grid or by allowing pedestrians to enter empty half cells. However, there is a price to pay: Obstacles cannot be placed freely which makes creating complex scenarios a challenge.

For the OSM with optimization on the circle, virtual pedestrians may still get stuck for a little while in front of the bottleneck (see Fig. 4(a)). The area in the opening where the floor field is lowest can be seen as a narrow ‘valley’. The optimization algorithm must find a point in an even smaller area, that is, on the intersection of the valley with the circle line. Typical optimization algorithms for one-dimensional problems, such as straight forward search on a grid or Brent’s method, may fail to find the optimum unless the grid or the algorithm is restarted several times for different starting points. This is computationally inefficient. In [28] the effect is mitigated by slightly disturbing the search grid in each iteration so that a more favorable point on the circle is always found after very few trials. Nonetheless this complete stop for one or few iterations seems unnatural.

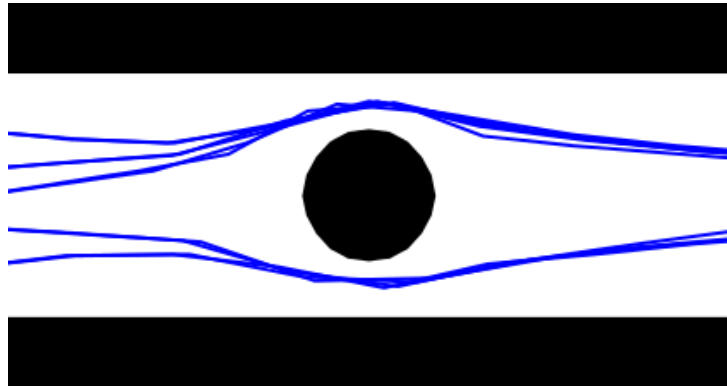
We would rather expect the pedestrians to make smaller, hesitant or adjustable steps that also lead to a speed reduction. In fact, the virtual pedestrians and the optimization algorithm face the same problem. The target



(a) Cellular Automaton

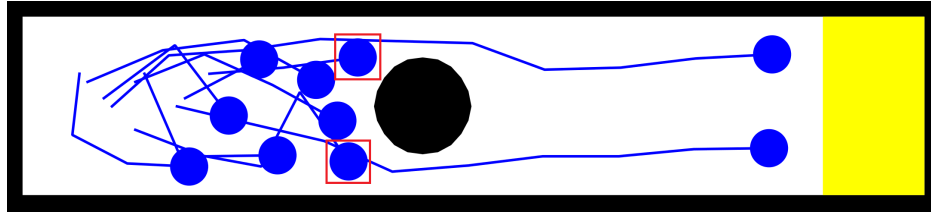


(b) Optimization on the circle

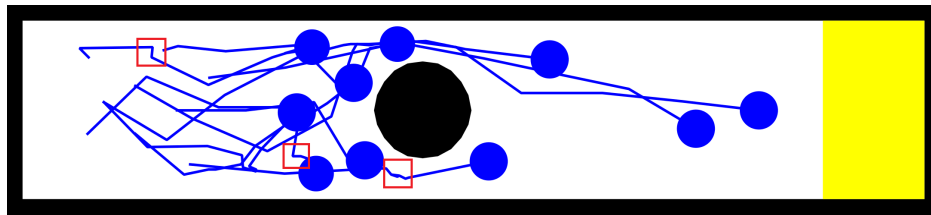


(c) Optimization on the disk

Figure 3: Navigation through a narrowing: Trajectories for single pedestrians passing from left to right. Pedestrians walk around a pillar; the opening between the wall and the pillar is exactly the torso diameter.



(a) Optimization on the circle: pedestrians get stuck for a while in front of the pillar (red rectangles) because of the small opening.



(b) Optimization on the disk: pedestrians make smaller, sometimes evasive steps (red rectangles) to navigate in crowded and difficult situations.

Figure 4: Navigation through a narrowing within a crowd: 10 Pedestrians start at once from left to right along a corridor with a pillar placed in the middle; the opening between the wall and the pillar is again exactly the torso diameter.

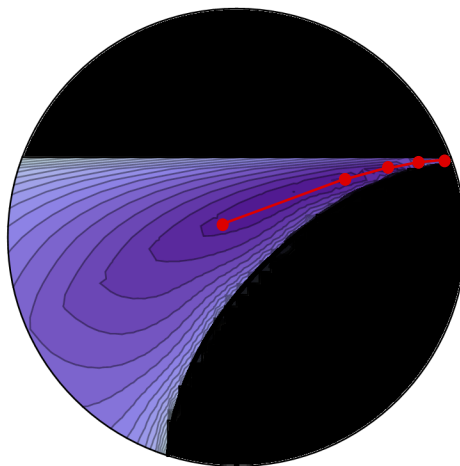


Figure 5: Sample path through the valley around the column with optimization on the disk in the OSM.

function, that is, the floor field is constructed in a way, that a narrow valley of lower values leads through the gap between column and wall. Using the whole disc as optimization area allows the numerical algorithm to slowly step forward within that valley (see Fig. 5). This matches the human behavior and, at the same time, ensures the success of the numerical solver, which was our goal.

5.2. *The density-speed relation*

The density-speed relation, expressed through fundamental diagrams, is a standard benchmark for the simulation of pedestrian movement: The denser the crowd, the slower overall movement becomes. The precise shape of the fundamental diagram depends on the context of the situation. E.g. do we model the rush hour at a German railway station or tourist traffic in, say, India? We refer to [31, 12, 23, 27, 5, 6] to see the present state of the discussion and conclude that we need the possibility to flexibly calibrate the model to any measured fundamental diagram [3, 5].

The numerical experiment follows the suggestions for test 10 in the RiMEA validation guideline [26]. Pedestrians walk through a corridor of length 30 m and width 4 m. At the end they are transported back to the start so that a perfect loop, without artifacts from corners, is formed. Mathematically this corresponds to periodic boundary conditions. The idea behind this construction is that, for each initial number of pedestrians in the corridor, a steady state solution should emerge where density and speed no longer change over time. This allows us to measure speed and density without worrying about local effects, at least for the numerical experiment.

We would like to point out that the same can never be expected for life measurements. That underlines the importance of calibration to any measured fundamental diagram within an acceptable error margin over accurate calibration to a particular diagram. Please refer to [6] for an in-depth discussion on robust calibration and, also, the need for sensitivity studies.

Social force type models [15] and cellular automata [5] need an extra speed adjustment algorithm to be able to fit a given density-speed curve. So does the OSM with optimization on a circle [28]. In all cases pedestrians are slowed down according to the density measured during the simulation run when the speed of the crowd surpasses the one given in the fundamental diagram, thus imposing the fundamental diagram from the outside. It is open to debate whether such an imposition is justified or whether calibration must be possible relying on the model parameters that deal with the pedestrians'

need for private space alone. Maybe the most significant advantage of the OSM with optimization on a disc is that we are capable of calibrating it by adapting the model parameters alone.

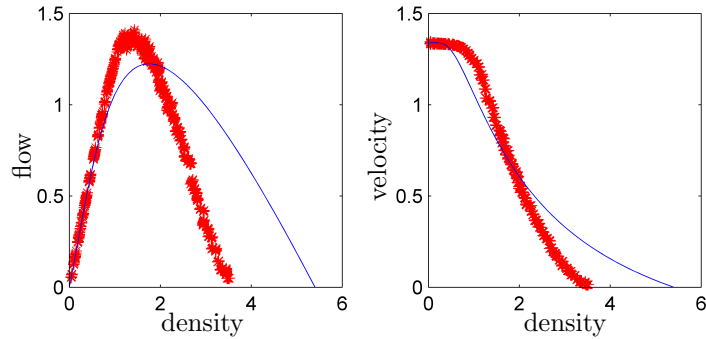
In Fig. 6 we compare simulation results for the two types of step-optimization in the OSM. In particular, the parameters for 'pedestrian avoidance' (see Eqn. 3) are those determined through calibrating the OSM with the stride adaptation on a disc.

We use Weidmann's reference curve from [36] to demonstrate the effect in Fig. 6. In 6(a) we observe a qualitative match. Pedestrians slow down with increasing density. However, the effect is overestimated and a realistic density of, say $5 \frac{\text{persons}}{\text{s}}$ before the crowd comes to a complete halt, is never reached. If one reduces the torso diameter, thus allowing a tighter packing of the crowd, the effect would be underestimated resulting in a curve above Weidmann's diagram. Only an imposed speed reduction, as described in [28] for the OSM with optimization on a circle or in [18] for a cellular automaton model, will allow a quantitative fit.

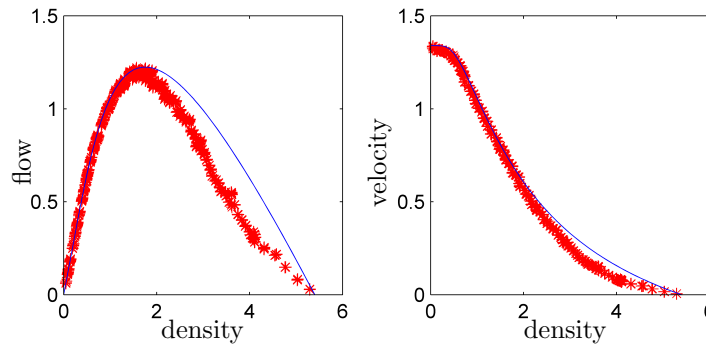
For the OSM with optimization on a disc, on the other hand, adjustment of the parameters for the avoidance of other pedestrians, that represent the need for personal space, suffices to achieve a good quantitative fit to Weidmann's diagram 6(b). This matches well with the idea that the differences between fundamental diagrams are caused by physical variations, such as the average fitness of people forming a crowd, as well as sociological and cultural variations in the need for personal space. There may be many more sources of influence. However, we believe the variations to be captured in the fundamental diagrams. Indian students, for example, showed a less pronounced need for personal space than German students in identical experiments described in [31, 3]. Also the fundamental diagrams measured at a major German railway station differed for a slow and, perhaps, tired early morning crowd and for faster commuters heading home in the evening rush hour [6].

6. Discussion and outlook

Pedestrian motion operates on a strategic, a tactical and an operational level [16]: When and where to do pedestrians decide to walk? How do they find their paths? How do they step forward? The Optimal Steps Model is a model for locomotion, that is, it describes the operational level. We believe that an inaccurate model of the operational level corrupts results on the higher levels. Examples are inaccuracies and oscillations as seen in



(a) OSM with optimization on the circle: Pedestrians move slower with increasing crowd density, but the maximum density where the crowd comes to a halt is underestimated. The solid (blue) line is Weidmann’s reference curve. The (red) crosses are results of computational experiments with varying crowd density.



(b) OSM with optimization on the disk. Pedestrians slow down by making smaller adjustive steps thus allowing the crowd to become more densely packed. A good quantitative match is achieved by adjusting solely the parameters capturing the need for personal space. The solid (blue) line is Weidmann’s reference curve. The (red) crosses are results of computational experiments with varying crowd density.

Figure 6: Density-speed relation: Adjustment to the (solid blue line) curve of Weidmann [36] with mean velocities (red crosses) of all pedestrians in simulation runs with different densities.

social force type models (see e.g. [4] or [21]) that may cause people to get stuck, lose their way, or hurry back and forth in a way that has no relation to meaningful strategic or tactical decisions. Grid restrictions as in cellular automata [19, 28] are just as undesirable because they limit the choice of directions and make it difficult to map a gradual compression of a crowd [35].

The problem goes even deeper. Humans neither move on smooth rails, nor do they hop from cell to cell. Instead they step forward in continuous space while instantly adapting their stride length and speed to the navigational situation. The simple extension of the Optimal Steps Model presented in this paper exactly maps this natural behavior. The mathematical formulation comes in the form of a two-dimensional optimization problem that can be solved successfully, and efficiently, with standard numerical algorithms. The success of the approach is reflected in the fact that calibration to measured density-speed relationships in a crowd is achieved simply by adjusting the need for personal space expressed through the pedestrian avoidance function. Forced deceleration as in [15] for social force models or [5] for cellular automata is no longer necessary to get a good quantitative fit to a given fundamental diagram. Also, the simulation results for important benchmark scenarios, such as navigation around a column in a narrow corridor and a crowd in front of a bottleneck, match reality much more closely than in the former state-of-the-art.

From a numerical analyst's point of view the model can be further improved by using smooth pedestrian and obstacle functions on a compact support as suggested for the Gradient Navigation Model in [7]. This will make the use of optimization algorithms possible that need first derivatives of the target function and may lead to improved computational speed. Also the search for neighbors can be accelerated by using linked-cell techniques.

However, our main goal was to provide an operational model that matches human locomotion to a significantly higher degree than the former state-of-the-art, eliminating typical artifacts known from social force type models or cellular automata, and thus providing a solid base for future work on the tactical and strategic level. Our vision is to incorporate sociological and psychological aspects into our model. The improved version of the Optimal Steps Model is the operational level that we will base our work on.

Acknowledgments

This work was funded by the German Federal Ministry of Education and Research through the project MEPKA on mathematical characteristics of pedestrian stream models (17PNT028).

References

- [1] Bar, M., July 2007. The proactive brain: using analogies and associations to generate predictions. *Trends in cognitive science* 11 (7), 280–289. URL http://suns.mit.edu/articles/Bar_TICS2007.pdf
- [2] Burstedde, C., Klauck, K., Schadschneider, A., Zittartz, J., 2001. Simulation of pedestrian dynamics using a two-dimensional cellular automaton. *Physica A: Statistical Mechanics and its Applications* 295, 507–525.
- [3] Chattaraj, U., Seyfried, A., Chakroborty, P., 2009. Comparison of pedestrian fundamental diagram across cultures. *Advances in Complex Systems* 12 (3), 393–405.
- [4] Chraïbi, M., Seyfried, A., Schadschneider, A., 2010. Generalized centrifugal-force model for pedestrian dynamics. *Physical Review E* 82 (4), 046111.
- [5] Davidich, M., Köster, G., 2012. Towards automatic and robust adjustment of human behavioral parameters in a pedestrian stream model to measured data. *Safety Science* 50 (5), 1253–1260.
- [6] Davidich, M., Köster, G., 12 2013. Predicting pedestrian flow: A methodology and a proof of concept based on real-life data. *PLoS ONE* 8 (12), 1–11.
- [7] Dietrich, F., 2013. An ode-based model for pedestrian motion and navigation. Bachelor’s thesis, Technische Universität München.
- [8] Ezaki, T., Yanagisawa, D., Ohtsuka, K., Nishinari, K., 2012. Simulation of space acquisition process of pedestrians using proxemic floor field model. *Physica A: Statistical Mechanics and its Applications* 391 (1–2), 291–299.

- [9] Gwynne, S., Galea, E., Owen, M., Lawrence, P., Filippidis, L., 1999. A review of the methodologies used in the computer simulation of evacuation from the built environment. *Building and Environment* 34 (6), 741–749.
URL <http://www.sciencedirect.com/science/article/pii/S0360132398000572>
- [10] Hartmann, D., 2010. Adaptive pedestrian dynamics based on geodesics. *New Journal of Physics* 12, 043032.
- [11] Helbing, D., Farkas, I., Vicsek, T., 2000. Simulating dynamical features of escape panic. *Nature* 407, 487–490.
- [12] Helbing, D., Johansson, A., Al-Abideen, H. Z., 2007. Dynamics of crowd disasters: An empirical study. *Physical Review E* 4 (4), 046109.
- [13] Helbing, D., Molnár, P., 1995. Social force model for pedestrian dynamics. *Physical Review E* 51 (5), 4282–4286.
- [14] Henein, C. M., White, T., 2007. Macroscopic effects of microscopic forces between agents in crowd models. *Physica A: Statistical Mechanics and its Applications* 373, 694 – 712.
- [15] Hoecker, M., Milbracht, P., 2009. Genetic algorithms as a means of adjusting pedestrian dynamics models. In: *Proceedings of the First International Conference on Soft Computing Technology in Civil, Structural and Environmental Engineering (CSC)*, Funchal, Madeira. p. 16.
- [16] Hoogendoorn, S. P., Bovy, P. H. L., 2004. Pedestrian route-choice and activity scheduling theory and models. *Transportation Research Part B: Methodological* 38 (2), 169–190.
URL <http://www.sciencedirect.com/science/article/pii/S0191261503000079>
- [17] Kirchner, A., Klüpfel, H., Nishinari, K., Schadschneider, A., Schreckenberg, M., 2003. Simulation of competitive egress behavior: comparison with aircraft evacuation data. *Physica A: Statistical Mechanics and its Applications* 324 (3–4), 689–697.

- [18] Klein, W., Köster, G., Meister, A., 2010. Towards the calibration of pedestrian stream models. In: Wyrzykowski, R., Dongarra, J., Karczewski, K., Wasniewski, J. (Eds.), *Parallel Processing and Applied Mathematics*. Springer, pp. 521–528.
- [19] Köster, G., Hartmann, D., Klein, W., 2011. Microscopic pedestrian simulations: From passenger exchange times to regional evacuation. In: Hu, B., Morasch, K., Pickl, S., Siegle, M. (Eds.), *Operations Research Proceedings 2010: Selected Papers of the Annual International Conference of the German Operations Research Society*. Springer, pp. 571–576.
- [20] Köster, G., Seitz, M., Treml, F., Hartmann, D., Klein, W., 2011. On modelling the influence of group formations in a crowd. *Contemporary Social Science* 6 (3), 397–414.
- [21] Köster, G., Treml, F., Gödel, M., 2013. Avoiding numerical pitfalls in social force models. *Physical Review E* 87 (6), 063305.
- [22] Lagarias, J. C., Reeds, J. A., Wright, M. H., Wright, P. E., 1998. Convergence properties of the nelder-mead simplex method in low dimensions. *SIAM Journal of Optimization* 9, 112–147.
- [23] Moussaïd, M., Helbing, D., Garnier, S., Johansson, A., Combe, M., Theraulaz, G., 2009. Experimental study of the behavioural mechanisms underlying self-organization in human crowds. *Proceedings of the Royal Society B: Biological Sciences* 276, 2755–2762.
URL <http://rspb.royalsocietypublishing.org/content/early/2009/05/07/rspb.2009.0405.abstract>
- [24] Moussaïd, M., Helbing, D., Theraulaz, G., 2011. How simple rules determine pedestrian behavior and crowd disasters. *Proceedings of the National Academy of Sciences* 108 (17), 6884–6888.
URL <http://www.pnas.org/content/108/17/6884.abstract>
- [25] Nelder, J. A., Mead, R., 1965. A simplex method for function minimization. *Computer Journal* 7, 308–313.
- [26] RiMEA, 2009. Richtlinie für Mikroskopische Entfluchtungsanalysen - RiMEA. RiMEA e.V., 2nd Edition.
URL <http://www.rimea.de/>

- [27] Schadschneider, A., Seyfried, A., 2011. Empirical results for pedestrian dynamics and their implications for modeling. *Networks and Heterogeneous Media* 6 (3), 545–560.
URL <http://aimsciences.org/journals/displayArticlesnew.jsp?paperID=6445>
- [28] Seitz, M. J., Köster, G., Oct 2012. Natural discretization of pedestrian movement in continuous space. *Physical Review E* 86, 046108.
- [29] Sethian, J. A., 1996. A fast marching level set method for monotonically advancing fronts. *Proceedings of the National Academy of Sciences* 93 (4), 1591–1595.
URL <http://www.pnas.org/content/93/4/1591.abstract>
- [30] Sethian, J. A., 1999. *Level Set Methods and Fast Marching Methods: Evolving Interfaces in Computational Geometry, Fluid Mechanics, Computer Vision, and Materials Science*. Cambridge University Press.
- [31] Seyfried, A., Steffen, B., Klingsch, W., Boltes, M., 2005. The fundamental diagram of pedestrian movement revisited. *Journal of Statistical Mechanics: Theory and Experiment* 2005 (10), P10002.
URL <http://stacks.iop.org/1742-5468/2005/i=10/a=P10002>
- [32] Smith, A., James, C., Jones, R., Langston, P., Lester, E., Drury, J., 2009. Modelling contra-flow in crowd dynamics dem simulation. *Safety Science* 47 (3), 395–404.
URL <http://www.sciencedirect.com/science/article/pii/S0925753508000799>
- [33] Treuille, A., Cooper, S., Popović, Z., 2006. Continuum crowds. *ACM Transactions on Graphics (SIGGRAPH 2006)* 25 (3), 1160–1168.
- [34] von Sivers, I., 2013. *Numerische Methoden zur Optimierung der Schritttrichtung und -weite in einem Modell der Personenstromsimulation*. Master’s thesis, Fernuniversität in Hagen.
- [35] Was, J., Lubas, R., 2013. Adapting social distances model for mass evacuation simulation, *journal of Cellular Automata*, Old City Publishing.

- [36] Weidmann, U., 1992. Transporttechnik der Fussgänger, 2nd Edition. Vol. 90 of Schriftenreihe des IVT. Institut für Verkehrsplanung, Transporttechnik, Strassen- und Eisenbahnbau (IVT) ETH, Zürich.
URL <http://e-collection.library.ethz.ch/view/eth:5929>
- [37] Zheng, X., Zhong, T., Liu, M., 2009. Modeling crowd evacuation of a building based on seven methodological approaches. Building and Environment 44 (3), 437–445.
URL <http://www.sciencedirect.com/science/article/pii/S0360132308000577>